XLI CILAMCE
XLI Ibero-Latin American Congress on Computational Methods in Engineering
16-19 November, 2020 FOZ DO IGUAÇU PARANÁ - BRAZIL

Nonlinear Receding Horizon Guidance of a Thrust-Vectoring Quadrotor Under Control Allocation Constraints

José Agnelo Bezerra[1], Davi A. Santos[1]

[1]*Dept. of Mechanical Engineering, Instituto Tecnológico de Aeronáutica*
Praça Marechal Eduardo Gomes, 50, Vila das Acácias, São José dos Campos/SP, Brazil
agnelo@ita.br, davists@ita.br

Abstract. The present work deals with the guidance of a pre-stabilized thrust-vectoring quadrotor, which is required to be steered from its initial condition to a given state-based wayset. To tackle this problem, we adopt a receding horizon strategy based on a constrained nonlinear programming, whose crucial constraints are the control mapping equation and the actuator limits. The online optimization solution is calculated using sequential quadratic programming. The proposed method is evaluated using computer simulation, which shows its effectiveness.

Keywords: Multirotor aerial vehicle, control allocation, wayset-based guidance, model predictive control.

1 Introduction

In the past few years, multirotor aerial vehicles (MAVs) have been employed in an increasing number of civilian applications, such as surveillance and remote sensing. For the near future, an intensive use in air transportation and goods delivery is expected. All the cited tasks especially demand high level of safety and maneuverability, so they can benefit from vehicles with full and redundant actuation. Such fully-actuated MAVs normally have a large number of rotors, which, in most cases, can be vectorable in one or two degrees of freedom (DOFs). For this reason, the control allocation of this class of vehicles deserves a particular attention.

In most of the papers devoted to the flight control of MAVs in general, the control allocation problem is solved by minimizing the total thrust magnitude command without considering the actuator limits [1–5]. Unfortunately, the optimal solution obtained in that way must be saturated inside an appropriate admissible set to avoid violating the actuator limits. The references [6, 7] avoid such saturations by formulating optimal control allocation problems that explicitly consider the actuator bounds as inequality constraints. However, it turns out that for an optimization-based control allocation problem to be feasible, it is necessary that the stabilization control laws provide them with admissible force and torque commands. This issue has not been investigated yet.

In particular, the present paper focus on a thrust-vectoring quadrotor vehicle in which each rotor has two vectoring DOFs. Differently from [6, 7], this work makes a step back proposing an outer-loop guidance that guarantees the feasibility of the optimal control allocation under actuator limits. This guidance problem is formulated using the receding horizon strategy based on a nonlinear constrained optimization that steers the MAV from its initial condition to a state-based wayset. The online nonlinear optimization is solved using sequential quadratic programming (SQP).

The remaining text is organized in the following manner: Section 2 describes the dynamics of a fully-actuated quadrotor and defines the guidance problem; Section 3 formulates the guidance strategy as a nonlinear optimization problem; Section 4 evaluates the proposed method using computer simulation; and Section 5 concludes the paper.

2 Problem Definition

In Subsection 2.1, a general form of the control mapping equation is presented. Subsection 2.2 describes the closed-loop modeling of an MAV. Finally, in Subsection 2.3, the guidance problem of this article is formulated.

2.1 Rotor Set Modeling

Consider a quadrotor and the Cartesian coordinate systems (CCSs) illustrated in Fig. 1. The four rotors of the vehicle are identical and can be controlled to tilt in two DOFs, besides the control of spinning rate. The *ground* CCS $\mathcal{S}_g \triangleq \{G; \hat{x}_g, \hat{y}_g, \hat{z}_g\}$ is fixed to the ground at a known point G. The *body* CCS $\mathcal{S}_b \triangleq \{B; \hat{x}_b, \hat{y}_b, \hat{z}_b\}$ is fixed to the airframe, with the origin at its center of mass B. Related to the ith rotor, $\mathcal{S}_{r_i} \triangleq \{R_i; \hat{x}_{r_i}, \hat{y}_{r_i}, \hat{z}_{r_i}\}$ and $\mathcal{S}_{b_i} \triangleq \{R_i; \hat{x}_{b_i}, \hat{y}_{b_i}, \hat{z}_{b_i}\}$ have both origin at the articulation point R_i, but $\mathcal{S}_{b_i}$ is fixed w.r.t. $\mathcal{S}_b$, while $\mathcal{S}_{r_i}$ is fixed w.r.t. rotor i. The orientation of $\mathcal{S}_{r_i}$ w.r.t. $\mathcal{S}_{b_i}$ can be parameterized by the vectoring angles $\varepsilon_i \in \mathbb{R}_+$ and $\eta_i \in \mathbb{R}_+$ using two consecutive elementary rotations around axes 1 and 2, respectively.

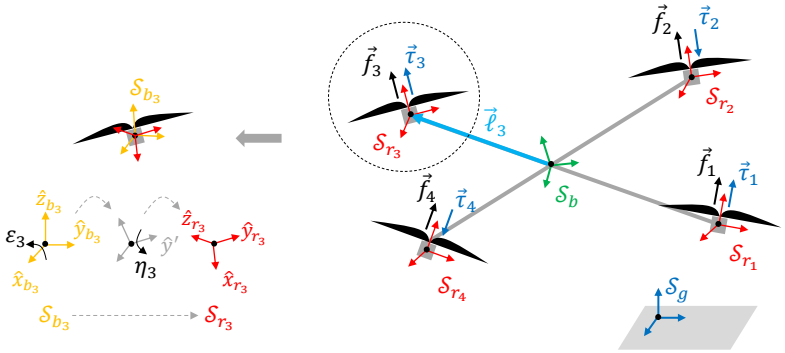

Figure 1. Schematic illustration of a quadrotor with two-DOF-vectoring rotors. In the left, it is presented a detail for the third rotor.

The aerodynamic thrust force and reaction torque produced by the ith propeller are modeled, respectively, by

$$\vec{f}_i = k^f \omega_i^2 \hat{z}_{r_i}, \tag{1}$$

$$\vec{\tau}_i = (-1)^{i+1} k^\tau \omega_i^2 \hat{z}_{r_i}, \tag{2}$$

where $\omega_i \in \mathbb{R}_+$ denotes the angular speed of the ith rotor, while $k^f, k^\tau \in \mathbb{R}_+$ are aerodynamic coefficients. Assume that ω_i is bounded according to

$$0 \leq \omega^{min} \leq \omega_i \leq \omega^{max}, \tag{3}$$

where $\omega^{min}, \omega^{max} \in \mathbb{R}_+$ are given physical parameters.

The resulting control force $\vec{f}^c$ and torque $\vec{\tau}^c$ produced by the rotors are given, respectively, by

$$\vec{f}^c = \sum_{i=1}^{4} \vec{f}_i, \tag{4}$$

$$\vec{\tau}^c = \sum_{i=1}^{4} (\vec{\tau}_i + \vec{\ell}_i \times \vec{f}_i), \tag{5}$$

where $\vec{\ell}_i$ is the (arm) vector from B to R_i.

Considering $\mathbf{f}_b^c, \boldsymbol{\tau}_b^c \in \mathbb{R}^3$ as the $\mathcal{S}_b$ representations of $\vec{f}^c$ and $\vec{\tau}^c$, respectively, the control vector $\mathbf{u} \in \mathbb{R}^6$ can be defined as follows

$$\mathbf{u} \triangleq (\mathbf{f}_b^c, \boldsymbol{\tau}_b^c) \tag{6}$$

Assume that $\mathbf{z}_i \in \mathbb{R}^3$ represents the thrust force $\vec{f}_i$ in $\mathcal{S}_{b_i}$. Then, it can be described by

$$\mathbf{z}_i = k^f \omega_i^2 \begin{bmatrix} \sin \eta_i \\ -\sin \varepsilon_i \cos \eta_i \\ \cos \varepsilon_i \cos \eta_i \end{bmatrix}. \tag{7}$$

Using the previous definition, Lemma 1 presents the control mapping equation in a linear form.

Lemma 1. The control mapping can be expressed as

$$\mathbf{u} = \mathbf{\Gamma}\mathbf{z} \tag{8}$$

where

$$\mathbf{z} \triangleq (\mathbf{z}_1, \mathbf{z}_2, \mathbf{z}_3, \mathbf{z}_4), \tag{9}$$

$$\mathbf{\Gamma} \triangleq \begin{bmatrix} \mathbf{D}^{b/b_1} & \mathbf{D}^{b/b_2} & \mathbf{D}^{b/b_3} & \mathbf{D}^{b/b_4} \\ \mathbf{M}_1\mathbf{D}^{b/b_1} & \mathbf{M}_2\mathbf{D}^{b/b_2} & \mathbf{M}_3\mathbf{D}^{b/b_3} & \mathbf{M}_4\mathbf{D}^{b/b_4} \end{bmatrix} \in \mathbb{R}^{6\times 12}, \tag{10}$$

$$\mathbf{M}_i \triangleq (-1)^{i+1}\frac{k^\tau}{k^f}\mathbf{I}_3 + [\boldsymbol{\ell}_{ib}\times] \in \mathbb{R}^{3\times 3}, \ \ \forall i \in \mathcal{I}_4, \tag{11}$$

with $\mathcal{I}_4 \triangleq \{1,2,3,4\}$, $\boldsymbol{\ell}_{ib}$ is the $\mathcal{S}_b$ representation of the arm vector $\vec{\ell}_i$ and $\mathbf{D}^{b/b_i} \in \mathrm{SO}(3)$ is the attitude matrix of $\mathcal{S}_b$ w.r.t. $\mathcal{S}_{b_i}$.

Proof. Equation (8) can be immediately obtained by representing eqs. (4) – (5) in $\mathcal{S}_b$ and rewriting the resulting equations into the desired matrix form. □

Finally, assume that the vectoring angles ε_i and η_i are bounded by

$$\varepsilon^{min} \leq \varepsilon_i \leq \varepsilon^{max}, \tag{12}$$

$$\eta^{min} \leq \eta_i \leq \eta^{max}, \tag{13}$$

where $\varepsilon^{min}, \eta^{min}, \varepsilon^{max}, \eta^{max} \in \mathbb{R}_+$ are given physical parameters.

2.2 Closed-Loop Dynamic Modeling

The state vector $\mathbf{x} \in \mathbb{R}^{12}$ and output vector $\mathbf{y} \in \mathbb{R}^6$ of the quadrotor can be defined as

$$\mathbf{x} \triangleq \left(\mathbf{r}_g^{b/g}, \boldsymbol{\alpha}^{b/g}, \mathbf{v}_g^{b/g}, \boldsymbol{\omega}_b^{b/g}\right), \tag{14}$$

$$\mathbf{y} \triangleq \left(\mathbf{r}_g^{b/g}, \boldsymbol{\alpha}^{b/g}\right), \tag{15}$$

where $\mathbf{r}_g^{b/g}, \mathbf{v}_g^{b/g} \in \mathbb{R}^3$ are, respectively, the position and velocity of $\mathcal{S}_b$ w.r.t. $\mathcal{S}_g$; $\boldsymbol{\alpha}^{b/g} \triangleq (\phi, \theta, \psi)$ is the attitude of $\mathcal{S}_b$ w.r.t. $\mathcal{S}_g$ expressed as Euler angles 1-2-3; and $\boldsymbol{\omega}_b^{b/g} \in \mathbb{R}^3$ represents the angular velocity of $\mathcal{S}_b$ w.r.t. $\mathcal{S}_g$.

Assume that $m \in \mathbb{R}_+$ is the total mass of the MAV, $\mathbf{J}_b \in \mathbb{R}^{3\times 3}$ represents its inertia matrix w.r.t. $\mathcal{S}_b$ and $g \in \mathbb{R}_+$ is the local gravity acceleration. Therefore, using the Newton-Euler equations, the translational and rotational dynamics can be modeled in the following state-space form

$$\dot{\mathbf{x}} = \mathbf{g}(\mathbf{x}) + \mathbf{B}(\mathbf{x})\,\mathbf{u}, \tag{16}$$

$$\mathbf{y} = \mathbf{C}\mathbf{x}, \tag{17}$$

where

$$\mathbf{g}(\mathbf{x}) \triangleq \begin{bmatrix} \mathbf{v}_g^{b/g} \\ \mathbf{M}(\boldsymbol{\alpha}^{b/g})\boldsymbol{\omega}_b^{b/g} \\ -g\mathbf{e}_3 \\ -\mathbf{J}_b^{-1}\left[\boldsymbol{\omega}_b^{b/g}\times\right]\left(\mathbf{J}_b\boldsymbol{\omega}_b^{b/g}\right) \end{bmatrix}, \mathbf{B}(\mathbf{x}) \triangleq \begin{bmatrix} \mathbf{0}_{3\times 3} & \mathbf{0}_{3\times 3} \\ \mathbf{0}_{3\times 3} & \mathbf{0}_{3\times 3} \\ \frac{1}{m}(\mathbf{D}^{b/g})^{\mathrm{T}} & \mathbf{0}_{3\times 3} \\ \mathbf{0}_{3\times 3} & \mathbf{J}_b^{-1} \end{bmatrix}, \mathbf{C} \triangleq \begin{bmatrix} \mathbf{I}_6 & \mathbf{0}_{6\times 6} \end{bmatrix},$$

$$\mathbf{M}(\boldsymbol{\alpha}^{b/g}) \triangleq \begin{bmatrix} \cos\psi/\cos\theta & -\sin\psi/\cos\theta & 0 \\ \sin\psi & \cos\psi & 0 \\ -\cos\psi\tan\theta & \sin\psi\tan\theta & 1 \end{bmatrix},$$

and $[\boldsymbol{\omega}_b^{b/g}\times] \in \mathbb{R}^{3\times 3}$ is the skew-symmetric matrix of $\boldsymbol{\omega}_b^{b/g}$ [8].

For the moment, it is assumed that a stabilizing flight control law is already available and has the general form

$$\mathbf{u} = \mathbf{h}\left(\mathbf{x}, \bar{\mathbf{y}}\right), \tag{18}$$

where $\bar{\mathbf{y}} \in \mathbb{R}^6$ is a command for $\mathbf{y}$ and $\mathbf{h} : \mathbb{R}^{12} \times \mathbb{R}^6 \to \mathbb{R}^6$ jointly describes the position and attitude control laws.

From equations (16) and (18), the closed-loop state equation is obtained as

$$\dot{\mathbf{x}} = \mathbf{g}^c\left(\mathbf{x}, \bar{\mathbf{y}}\right), \tag{19}$$

where $\mathbf{g}^c\left(\mathbf{x}, \bar{\mathbf{y}}\right) \triangleq \mathbf{g}\left(\mathbf{x}\right) + \mathbf{B}\left(\mathbf{x}\right)\mathbf{h}\left(\mathbf{x}, \bar{\mathbf{y}}\right)$.

2.3 MAV Guidance Problem

Define a wayset $\mathcal{W} \subset \mathbb{R}^{12}$ as a given symmetric, compact, and convex set and the corresponding waypoint $\mathbf{w} \in \mathbb{R}^{12}$ as its center. The wayset $\mathcal{W}$ is the input of the guidance law.

The main problem of this paper is stated below.

Problem 1. The MAV guidance problem is to design a guidance law $\bar{\mathbf{y}}\left(\mathbf{x}, \mathcal{W}\right)$ which steers the closed-loop system described by (19) from the initial condition $\mathbf{x}(t_0)$ to a given wayset $\mathcal{W}$, while satisfying the control mapping equation (8) and respecting the actuator bounds (3), (12), (13).

3 Problem Solution

By replacing the inequalities (3), (12), and (13) into equation (7), we can obtain an admissible set $\mathcal{Z} \subset \mathbb{R}^3$ for the rotor thrust $\mathbf{z}_i$. In this paper, we approximate this set by a polytopic subset, which can be described by the inequality

$$\mathbf{\Lambda}_i \mathbf{z}_i \leq \boldsymbol{\lambda}_i, \tag{20}$$

where $\mathbf{\Lambda}_i \in \mathbb{R}^{p\times 3}$ and $\boldsymbol{\lambda}_i \in \mathbb{R}^p$, for $p \in \mathbb{Z}_+$, are given.

Therefore, using (9) and (20), we obtain

$$\mathbf{\Lambda}\mathbf{z} \leq \boldsymbol{\lambda}, \tag{21}$$

with $\mathbf{\Lambda} \in \mathbb{R}^{4p\times 12}$ and $\boldsymbol{\lambda} \in \mathbb{R}^{4p}$.

A discrete time model related to the closed loop dynamics in (19) can be obtained by using the zero-order hold approach with sampling time $t^s \in \mathbb{R}_+$

$$\mathbf{x}_{k+1} = \mathbf{g}^d\left(\mathbf{x}_k, \bar{\mathbf{y}}_k\right), \tag{22}$$

where $\mathbf{g}^d : \mathbb{R}^{12} \times \mathbb{R}^6 \to \mathbb{R}^{12}$ is calculated by the integration of $\mathbf{g}^c$ and $\mathbf{x}_k \in \mathbb{R}^{12}$, $\bar{\mathbf{y}}_k \in \mathbb{R}^6$ are, respectively, the state and output command on the discrete time $k \in \mathbb{Z}_+$.

The receding horizon strategy is adopted to solve Problem 1. The embedded optimization, at instant k, is formulated as

$$\{\bar{\mathbf{y}}_j^*\} = \quad \arg\min \quad \sum_{j=0}^{N-1} \left(\|\mathbf{x}_{j+1} - \mathbf{w}\|^2 + \rho\|\mathbf{z}_j - \mathbf{z}^{\text{ref}}\|^2\right) \tag{23}$$

$$\text{s.t.}, \forall j \in \mathcal{I}_N \quad \mathbf{x}_0 = \mathbf{x}_k, \tag{24}$$

$$\mathbf{x}_{j+1} = \mathbf{g}^d\left(\mathbf{x}_j, \bar{\mathbf{y}}_j\right), \tag{25}$$

$$\mathbf{h}\left(\mathbf{x}_j, \bar{\mathbf{y}}_j\right) - \mathbf{\Gamma}\mathbf{z}_j = 0, \tag{26}$$

$$\mathbf{\Lambda}\mathbf{z}_j - \boldsymbol{\lambda} \leq 0, \tag{27}$$

$$\mathbf{x}_N \in \mathcal{W}, \tag{28}$$

where $\mathcal{I}_N \triangleq \{0, 1, \ldots, N-1\}$, $N \in \mathbb{Z}_+$ is the prediction horizon and $\rho \in \mathbb{Z}_+$ is a given weight related to the actuation efforts. The sequence $\{\bar{\mathbf{y}}_j^*\}$ represents the optimal trajectory calculated for $\bar{\mathbf{y}}_j$, with $j \in \mathcal{I}_N$, and $\mathbf{z}^{\text{ref}} \in \mathbb{R}^{12}$ is the reference value for $\mathbf{z}$, which is given for the quadrotor in hover condition, with non-vectored rotors.

To solve the previous nonlinear optimization problem online, it is approximated to simpler quadratic subproblems, using the SQP algorithm. So, employing the receding horizon strategy, only the first optimal input of the sequence $\{\bar{\mathbf{y}}_j^*\}$ is applied to the system, *i.e.*, $\bar{\mathbf{y}}_k = \bar{\mathbf{y}}_0^*$. Therefore, at the next discrete time, a new state measurement $\mathbf{x}_{k+1}$ is obtained and the whole process is repeated.

4 Simulation Results

The proposed method is illustrated for a x-shaped fully-actuated quadrotor via simulation, which was performed in MATLAB, using the Euler integrator, with time step of $0.001\,\mathrm{s}$. The considered parameters of the vehicle are the following: $m = 2.132\,\mathrm{kg}$, $\mathbf{J}_b = \mathrm{diag}([0.043, 0.055, 0.092])\mathrm{kg\,m^2}$, $\ell = 0.36\,\mathrm{m}$, $k^f = 2.532 \times 10^{-5}\,\mathrm{kg\,m}$, $k^\tau = 5.997 \times 10^{-7}\,\mathrm{kg\,m^2}$, $\omega^{max} = 754\,\mathrm{rad/s}$, $\omega^{min} = 0$, $\varepsilon^{max} = \eta^{max} = \pi/2\,\mathrm{rad}$ and $\varepsilon^{min} = \eta^{min} = -\pi/2\,\mathrm{rad}$.

The flight control of eq. (18), as done in [1], was implemented using two stabilizing control laws, respectively for attitude and position dynamics

$$\boldsymbol{\tau}_b^c = \mathbf{J}_b \left[k_1 \left(\bar{\boldsymbol{\alpha}}^{b/g} - \boldsymbol{\alpha}^{b/g} \right) - k_2 \boldsymbol{\omega}_b^{b/g} \right] + \left[\boldsymbol{\omega}_b^{b/g} \times \right] \left(\mathbf{J}_b \boldsymbol{\omega}_b^{b/g} \right), \tag{29}$$

$$\mathbf{f}_g^c = m \left[k_3 \left(\bar{\mathbf{r}}_g^{b/g} - \mathbf{r}_g^{b/g} \right) - k_4 \mathbf{v}_g^{b/g} + g \mathbf{e}_3 \right], \tag{30}$$

where $k_1, k_2, k_3, k_4 \in \mathbb{R}_+$ are design parameters and the commands $\bar{\boldsymbol{\alpha}}^{b/g}, \bar{\mathbf{r}}_g^{b/g}$ yield from $\bar{\mathbf{y}}$, *i.e.*, $\bar{\mathbf{y}} = (\bar{\mathbf{r}}_g^{b/g}, \bar{\boldsymbol{\alpha}}^{b/g})$.

The nonlinear optimization problem described in (23)–(28) is solved using the *fmincon* function with the SQP algorithm, which is provided by the Optimization Toolbox of MATLAB. The considered parameters of the guidance and control laws are the following: $t^s = 0.1\,\mathrm{s}$, $N = 20$, $\rho = 0.01$, $k_1 = k_3 = 225\,\mathrm{s}^{-2}$ and $k_2 = k_4 = 30\,\mathrm{s}^{-1}$.

To visualize the effectiveness of the guidance strategy, two scenarios were tested: **Scenario A** simulates the system with the proposed guidance, while, in **Scenario B**, the method is not used and the waypoint **w** is passed to the flight control as a step command. In both scenarios, it is considered a position tracking mission, with the quadrotor starting on $[0, 0, 1]^\mathrm{T}$ and the waypoint is $[1, 0, 1]^\mathrm{T}$, both conditions with null attitude and velocities.

The Fig. 2 presents the quadrotor states through the time. It is worth mentioning that some states were omitted, since they remain close to the related initial condition. One may observe, in both scenarios, that all the states are successfully driven into the target set. In Scenario B, the quadrotor reaches the wayset much faster than Scenario A, which is a result of the actuator constraint (27) considered in the guidance strategy.

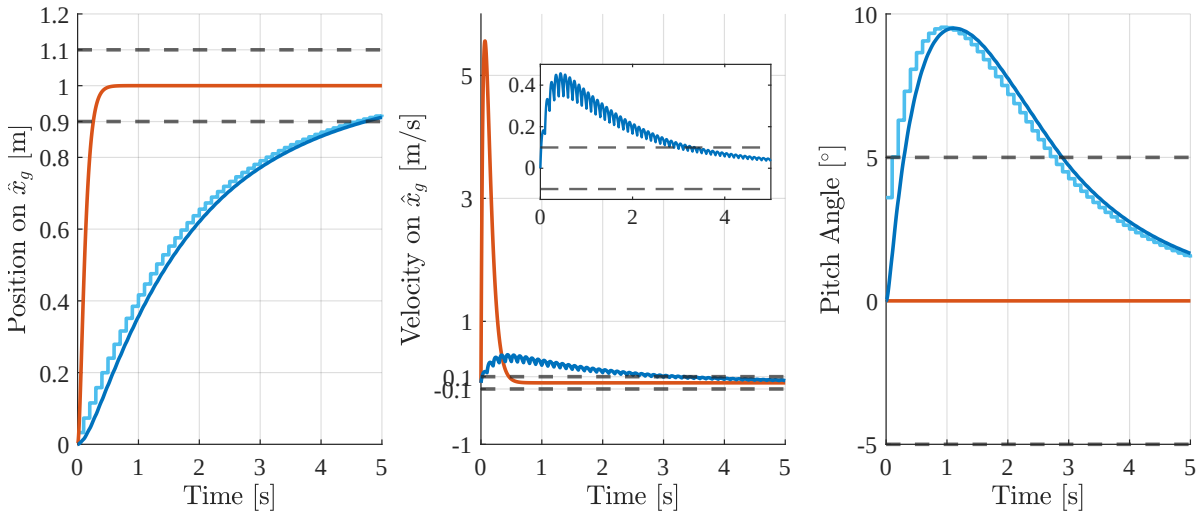

Figure 2. States of the quadrotor during the simulation. Related to Scenario A, the cyan lines represent the guidance commands, while the blue ones indicate the states values. The red lines illustrate the states simulated in Scenario B and the dashed lines represent the limits of the respective waysets.

The Fig. 3 shows the actuation variables related to the second rotor of the MAV. The other rotors have similar behaviors and are omitted for brevity. One may observe, in Scenario B, that the upper bound of the spinning velocity ω_2 is violated. Conversely, in Scenario A, the proposed method prevents this violation and respects the physical bounds of the actuators with large margins.

5 Conclusions

This paper proposes a receding horizon guidance that directly considers the control mapping equation and the actuator limits. As the method yields a nonlinear optimization problem, it is approximated for solution, so one

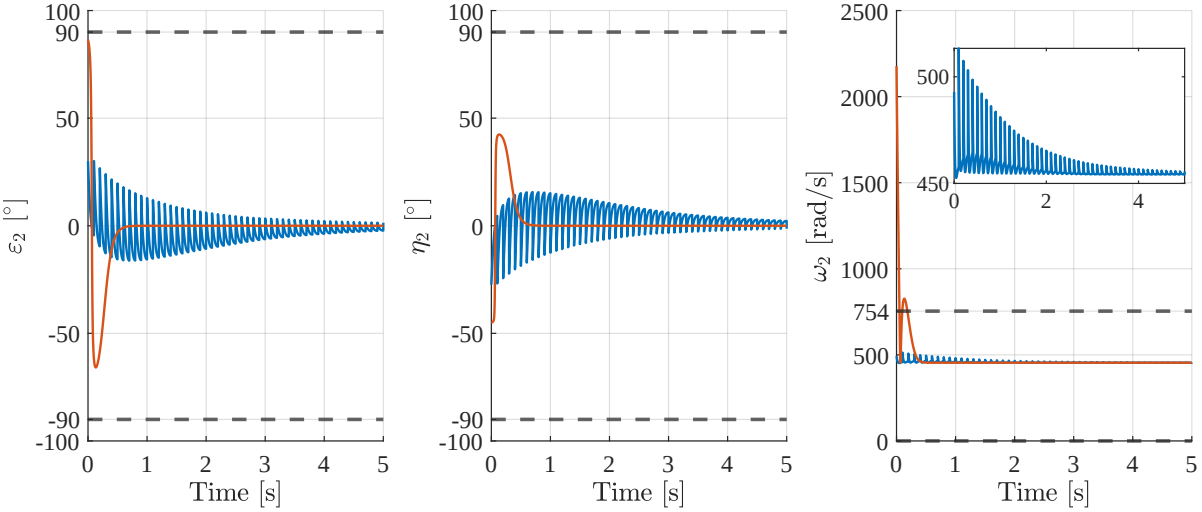

Figure 3. Actuation variables related to the second rotor of the MAV. The blue lines illustrate the results of Scenario A, while the red lines represent Scenario B and the dashed lines determine the bounds of the respective variables.

could expect that the approximations would induce some lack of accuracy in satisfying the constraints. However, the simulation of a wayset tracking mission shows that the actuator bounds are strictly respected. This preliminary result encourages to deeply investigate the properties of the method and to simulate its application to different scenarios.

Acknowledgements. The authors would like to thank the São Paulo Research Foundation (FAPESP), for the financial support under grant 2019/05334-0. The second author is also grateful for the support of the Brazilian National Council for Scientific and Technological Development (CNPq), under grant 302637/2018-4.

Authorship statement. The authors hereby confirm that they are the sole liable persons responsible for the authorship of this work, and that all material that has been herein included as part of the present paper is either the property (and authorship) of the authors, or has the permission of the owners to be included here.

References

[1] Diógenes, H. B. & Santos, D. A., 2017. Dynamic Modeling and Control of a Quadcopter with Longitudinal-Tilting Rotors. In *XXXVIII Iberian Latin American Congress on Computational Methods in Engineering*, Florianópolis, Brazil.
[2] Ducard, G. J. J. & Hua, M.-D., 2011. Discussion and Practical Aspects on Control Allocation for a Multi-Rotor Helicopter. In *ISPRS - International Archives of the Photogrammetry, Remote Sensing and Spatial Information Sciences*, pp. 95–100, Zurich, Switzerland.
[3] Ryll, M., Bicego, D., Giurato, M., Lovera, M., & Franchi, A., 2020. Fast-hex – a morphing hexarotor: Design, mechanical implementation, control and experimental validation.
[4] Arellano-Quintana, V. M., Merchan-Cruz, E. A., & Franchi, A., 2018. A novel experimental model and a drag-optimal allocation method for variable-pitch propellers in multirotors. *IEEE Access*, vol. 6, pp. 68155–68168.
[5] Long, Y., Wang, L., & Cappelleri, D. J., 2014. Modeling and global trajectory tracking control for an over-actuated mav. *Advanced Robotics*, vol. 28, n. 3, pp. 145–155.
[6] Monteiro, J. C., Lizarralde, F., & Hsu, L., 2016. Optimal control allocation of quadrotor UAVs subject to actuator constraints. In *2016 American Control Conference (ACC)*, pp. 500–505, Boston, USA.
[7] Smeur, E., Hoppener, D., & Wagter, C. D., 2017. Prioritized Control Allocation for Quadrotors Subject to Saturation. In *International Micro Air Vehicle Conference and Flight Competition (IMAV) 2017*, pp. 37–43, Toulouse, France.
[8] Shuster, M. D., 1993. A Survey on Attitude Representations. *Journal of the Astronautical Sciences*, vol. 41, n. 4, pp. 439–517.